Understanding the interaction of an antitumoral platinum(II) 7-azaindolate complex with proteins and DNA

ARTICLE *in* BIOMETALS · AUGUST 2014

Impact Factor: 2.5 · DOI: 10.1007/s10534-014-9780-1 · Source: PubMed

11 AUTHORS, INCLUDING:

Silvia Atrian
University of Barcelona
123 PUBLICATIONS **3,295** CITATIONS
SEE PROFILE

Jean-Didier Maréchal
Autonomous University of Barcelona
75 PUBLICATIONS **1,056** CITATIONS
SEE PROFILE

Merce Capdevila
Autonomous University of Barcelona
99 PUBLICATIONS **1,849** CITATIONS
SEE PROFILE

Jose Ruiz
University of Murcia
90 PUBLICATIONS **1,820** CITATIONS
SEE PROFILE

Biometals
DOI 10.1007/s10534-014-9780-1

Understanding the interaction of an antitumoral platinum(II) 7-azaindolate complex with proteins and DNA

Katia G. Samper · Venancio Rodríguez · Elisabeth Ortega-Carrasco · Sílvia Atrian · Jean Didier Maréchal · Natalia Cutillas · Ana Zamora · Concepción de Haro · Mercè Capdevila · José Ruiz · Òscar Palacios

Received: 22 May 2014 / Accepted: 25 July 2014

Abstract The reactivity of the [Pt(dmba)(aza-N1)(dmso)] complex **1**, (a potential antitumoral drug with lower IC_{50} than cisplatin in several tumoral cell lines) with different proteins and oligonucleotides is investigated by means of mass spectrometry (ESI-TOF MS). The results obtained show a particular binding behaviour of this platinum(II) complex. The interaction of **1** with the assayed proteins apparently takes place by Pt-binding to the most accessible coordinating amino acids, presumably at the surface of the protein -this avoiding protein denaturation or degradation- with the subsequent release of one or two ligands of **1**. The specific reactivity of **1** with distinct proteins allows to conclude that the substituted initial ligand (dmso or azaindolate) is indicative of the nature of the protein donor atom finally bound to the platinum(II) centre, *i.e.* N- or S-donor amino acid. Molecular modeling calculations suggest that the release of the azaindolate ligand is promoted by a proton transfer to the non-coordinating N present in the azaindolate ring, while the release of the dmso ligand is mainly favoured by the binding of a deprotonated Cys. The interaction of complex **1** with DNA takes always place through the release of the azaindolate ligand. Interestingly, the interaction of **1** with DNA only proceeds when the oligonucleotides are annealed forming a double strand. Complex **1** is also capable to displace ethidium bromide from DNA and it also weakly binds to DNA at the minor groove, as shown by Hoechst 33258 displacement experiments. Furthermore, complex **1** is also a good inhibitor of cathepsin B (an enzyme implicated in a number of cancer related events). Therefore, although compound **1** is definitely able to bind proteins that can hamper its arrival to the nuclear target, it should be taken into consideration as a putative anticancer drug due to its strong interaction with oligonucleotides and its effective inhibition of cat B.

Keywords Antitumoral compound · Platinum · DNA interaction · Protein interaction · Mass spectrometry

Electronic supplementary material The online version of this article (doi:10.1007/s10534-014-9780-1) contains supplementary material, which is available to authorized users.

K. G. Samper · E. Ortega-Carrasco · J. D. Maréchal · M. Capdevila · Ò. Palacios (✉)
Departament de Química, Facultat de Ciències, Universitat Autònoma de Barcelona, Cerdanyola del Vallès, 08193 Barcelona, Spain
e-mail: Oscar.Palacios@uab.cat

V. Rodríguez · N. Cutillas · A. Zamora · C. de Haro · J. Ruiz
Departamento de Química Inorgánica, Universidad de Murcia, 30071 Murcia, Spain

V. Rodríguez · N. Cutillas · A. Zamora · C. de Haro · J. Ruiz
Instituto Murciano de Investigación Biosanitaria (IMIB), Murcia, Spain

S. Atrian
Departament de Genètica, Facultat de Biologia, Universitat de Barcelona, 08028 Barcelona, Spain

Published online: 09 August 2014

Abbreviations

aza	7-Azaindolate
cat B	Cathepsin B
Cyt C	Cytochrome C
Dmba	*N,N*-dimethylbenzylamine-κ*N*,κ*C*
Dmso	Dimethylsulfoxide
DS	Double strand oligonucleotide
EB	Ethidium bromide
HSA	Human serum albumin
MT1	Zn_7-MT complex of the recombinant mouse metallothionein isoform 1
Myo	Myoglobin
SS	Single strand oligonucleotide
Tf	Transferrin

Introduction

Since the end of the 70 s, platinum-based complexes, such as cisplatin, carboplatin and oxaliplatin have resulted the most effective treatments against cancer (Lippert 1999; Jakupec et al. 2008; Harper et al. 2010). Their clinical success has promoted the design of further generations of Pt drugs aiming at overcoming several drawbacks (Barnes and Lippard 2004), like severe side-effects, the intrinsic resistance of some tumors, and the development of resistance induced after initial treatment (Jakupec et al. 2008). The mechanism of platinum-anticancer drugs involves their binding to DNA (Jamieson and Lippard 1999), which induces structural modifications on the double helix leading to apoptosis (Lippert 1999). The natural ability of cells to prevent toxicity promotes several responses: changes in the intracellular accumulation of the drug; increased production of intracellular thiols; increased capability of cells to repair platinum-induced DNA damage; and failure to initiate apoptosis in the presence of platinated DNA (Paolicchi et al. 2002). Due to the strong reactivity of platinum compounds toward S-donor molecules, which leads to the formation of very stable Pt^{II}-thiolate bonds, various kinds of intracellular thiol-rich molecules, as metallothioneins, account for conferring resistance to antitumor platinum drugs through their competition with DNA (Knipp et al. 2007). Also the interaction of the platinum drugs with other proteins may play crucial roles in their uptake and biodistribution processes, as well as in determining their toxicity profile, as they are the first potential interaction partners in the blood stream after intravenous administration (Barnes and Lippard 2004).

Therefore, decoding how platinum(II) complexes interact with proteins is key for designing new effective drugs. The contribution of electrospray ionization mass spectrometry (ESI–MS) to monitor such interaction has been proven to be extremely valuable when using, either nano-ESI sources, which are common in the study of the interaction of platinum drugs with proteins (Egger et al. 2008; Montero et al. 2007), or conventional ESI sources (Samper et al. 2012 and others), which, unlike the nano-ESI sources, allow to work under a wide set of experimental conditions.

The synthesis and X-ray crystal structure of a dmba-based platinum complex **1**, [Pt(dmba)(aza-N1)(dmso)], (dmba = *N,N*-dimethylbenzylamine-κ*N*, κ*C*; aza-N1 = 7-azaindolato-κ*N*1; dmso = dimethylsulfoxide-κ*S*), have been reported (Ruiz et al. 2010). Complex **1** not only contains a chelating ligand forming a very stable C–Pt bond (which accounts for the integrity of the Pt moiety), but also shows submicromolar activity both in A2780 and T47D cell lines (IC_{50} = 0.34 μM and 0.53 μM, respectively). Additionally, it exhibits very low resistance factors in the A2780 cell line, which has acquired resistance to cisplatin. Finally, the formation of adducts of this platinum(II) complex **1** with calf thymus DNA, followed by circular dichroism, has suggested important and promising modifications in the secondary structure of DNA, which point out the putative interest of this complex as an anticancer drug (Ruiz et al. 2010).

In this work we have studied the interaction of complex **1** with several proteins (albumin, transferrin, myoglobin -as a model for haemoglobin-, cytochrome C, and metallothionein -mammalian MT1) that can easily interact with metallic drugs after its administration in the blood stream and before their arrival to the putative target (*i.e.* the cellular nucleus). These interactions have been monitored by an ESI-TOF MS instrument equipped with a conventional ESI source and with a high resolution TOF analyzer. ESI–MS has also been used to monitor the interaction of complex **1** with a designed double-stranded oligonucleotide containing the GG Pt-binding site motif. To further investigate

the binding mode between complex **1** and DNA, fluorescence competition experiments with ethidium bromide (EB) and Hoechst 33258 were carried out. The particular behaviour observed in the interaction of complex **1** with both kinds of biomolecules, proteins and oligonucleotides, made necessary the use of theoretical calculations in order to better rationalize the origin of its reactivity. The specific interaction of **1** with MT1 -a common target for Pt^{II} compounds- has also been further investigated by optical spectroscopy. Finally, the inhibitory effect of complex **1** on cathepsin B (cat B) -an abundant and ubiquitously expressed cysteine peptidase whose increased expression and secretion have been related to tumoral cell migration and invasion capacity (Fernandez et al. 2001)- has been evaluated.

Experimental section

Synthesis and characterization of the Pt complex **1**

The synthesis and full characterization of the [Pt(dmba)(aza-N1)(dmso)] complex used in this work, hereafter denoted as **1**, was already described (Ruiz et al. 2010). The 3D structure determined by X-ray diffraction allowed to prove the coordination environment of the Pt^{II} centre shown in Fig. 1.

Due to the neutral nature of **1**, which is responsible of its relatively low solubility in water, the complex was dissolved in dimethylsulfoxide (dmso).

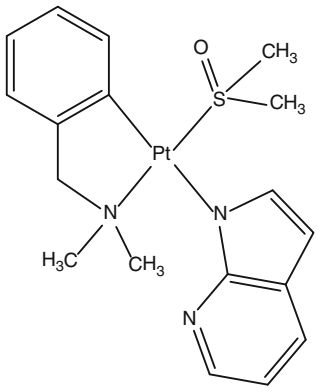

$C_{18}H_{23}N_3OSPt$

MW: 524.54 g/mol

Fig. 1 Schematic representation of the [Pt(dmba)(aza-N1)(dmso)] complex used in this work, based on X-ray diffraction (from ref. (Castillo-Busto et al. 2009))

Sample preparation and incubation previous to mass spectrometry analysis

Most of the proteins used in this work were purchased from Sigma-Aldrich: human serum albumin (A8763), transferrin (T3309), myoglobin (M6036) and cytochrome C (C3484). Mammalian metallothionein (mouse MT1 isoform) was recombinantly produced as a Zn-complex in *E. coli*, and fully characterized as previously reported (Cols et al. 1997). Several 1-mM solutions of each protein (except for MT1) were prepared in water by weighting the corresponding lyophilized protein. The purified recombinant preparations of MT1 consisted on Zn_7-MT1 complexes in a 50 mM Tris-$HClO_4$ solution at pH 7.0, and of a 0.275 mM protein concentration. Additionally, a 5-mM solution of **1** in dmso was prepared.

From all these starting solutions, 100-µL samples of 100-µM protein solutions were prepared by mixing the appropriate volume of each protein solution with the dmso solution of **1** to render preparations at the desired protein:Pt molar ratios (1:1, 1:5, 1:10) in 25 mM ammonium bicarbonate buffer at pH 7. The final solutions contained a 2 % concentration of dmso to keep the complex soluble Afterwards, the incubation of these mixtures was performed at 37 °C for 24 or 48 h in a stirring water bath.

The complementary single strand (SS) oligonucleotides used in this work, OP1 and OP2 (Table 1), were purchased from Eurofins MWG Synthesis GmbH (Ebersberg, Germany). In order to obtain the corresponding double-stranded (DS) oligonucleotide, equimolar quantities of each oligonucleotide (50 µM solutions in 25 mM ammonium bicarbonate buffer at pH 7.0) were incubated at 70 °C for 2 h and allowed to cool at room temperature overnight.

The SS and DS oligonucleotides were analyzed by ESI-TOF MS in negative mode as already described (Samper et al. 2012). These measurements confirmed the purity and identity of the single-stranded OP1 and OP2 oligonucleotides (Table 1), and allowed to observe the formation of the double-stranded oligonucleotide, which has been proved to be stable under the ESI–MS conditions assayed. The mass spectra obtained after incubation of equimolar amounts of the complementary OP1 and OP2 oligonucleotides showed a peak corresponding to the DS with similar intensity to those related to the single oligonucleotides, which suggested an efficiency of 50 % in their

Table 1 Sequences and experimental molecular weight (MW) of the single (SS) and double (DS) stranded oligonucleotides determined by ESI–MS (Casini et al. 2008). The experimental error was always lower than 0.1 %

	Name	Sequence	Experimental MW (Da)	Theoretical MW (Da)
SS	OP1	5′-CACTTCCGCT-3′	2,938.6	2,938.97
	OP2	5′-AGCGGAAGTG-3′	3,116.6	3,117.10
DS			6,055.2	6,056.07

annealing reaction (Samper et al. 2012). This result was also confirmed by size exclusion-HPLC–UV.

Following an analogous procedure to that described above for the proteins, 100-μL samples, containing the appropriate amounts of the DS obtained and complex **1**, in order to reach a 20 μM concentration of DS and the desired DS:Pt molar ratios (1:1, 1:5, 1:10) were prepared. The mixtures were afterwards incubated at 37 °C for 24 or 48 h in a stirring water bath.

For the mass measurements, all the oligonucleotides-containing preparations were adequately diluted in order to reach the best S/N ratio in the mass spectra, at the chosen working conditions.

Mass spectrometry conditions

Molecular mass determinations were performed by electrospray ionization mass spectrometry equipped with a time-of-flight analyzer (ESI-TOF MS) using a Micro Tof-Q Instrument (Bruker Daltonics GmbH, Bremen, Germany) calibrated with ESI-L Low Concentration Tuning Mix (Agilent Technologies), interfaced with a Series 1100 HPLC pump (Agilent Technologies) equipped with an autosampler, both controlled by the Compass Software.

The interaction of the platinum(II) complex **1** with proteins was analyzed in positive mode under the following experimental conditions: 20 μL of the sample were injected at 40 μL min^{-1}; the capillary-counterelectrode voltage was 4.5 kV; the desolvation temperature was 100 °C; dry gas at 6 L min^{-1}. Spectra were collected throughout a m/z range from 800 to 2500. The liquid carrier was a 85:15 mixture of 15 mM ammonium acetate and acetonitrile, pH 7.0.

The interaction of the platinum(II) complex **1** with the OP1, OP2 and DS oligonucleotides was analyzed in negative mode under the following experimental conditions: 10 μL of the sample were injected at 40 μL min^{-1}; the capillary-counterelectrode voltage was 3.9 kV; the desolvation temperature was 100 °C; dry gas at 6 L min^{-1}. Spectra were collected throughout a m/z range from 800 to 2500. The liquid carrier was a 90:10 mixture of 15 mM ammonium acetate and acetonitrile, pH 7.0.

All samples were injected at least in duplicate to ensure reproducibility.

HPLC separation

HPLC was performed with a Series 1200 HPLC pump (Agilent Technologies, Santa Clara, CA, USA) equipped with an autosampler and a diode array detector, all controlled by the Compass Software. 100-μL aliquots of the samples were injected into a Superdex Peptide column (GE Healthcare, Fairfield, CT, USA) and eluted with 50 mM ammonium bicarbonate buffer at pH 7.5, at a flow rate of 550 μL min^{-1}. At the exit of the column, the absorbance was recorded at 210, 254, and 280 nm. Each of the peaks detected (due to DS, OP1, and OP2) were separately collected and all the fractions corresponding to a same peak were pooled and the sample homogenized before incubation with the Pt^{II} complex.

Optical spectroscopy

Circular dichroism (CD) spectroscopy was performed using a model J-715 spectropolarimeter (JASCO, Gross-Umstadt, Germany) equipped with a computer (J-700 software, JASCO). Measurements were carried out at a constant temperature of 25 °C maintained by a Peltier PTC-351 S apparatus (TE Technology Inc., Traverse City, MI, USA). Electronic absorption was measured on an HP-8453 diode-array UV–vis spectrophotometer (GMI Inc., Ramsey, MN, USA), using 1-cm capped quartz cuvettes, and correcting for the dilution effects by means of the GRAMS 32 software (Thermo Fisher Scientific Inc., Waltham, MA, USA). Fluorescence measurements were carried out with a Perkin-Elmer LS 55 50 Hz Fluorescence Spectrometer

under different working conditions, depending on the experiment carried out.

Ethidium bromide and Hoechst 33258 displacement experiments

In the ethidium bromide (EB) fluorescence displacement experiment, a 3-mL solution containing 10 μM calf thymus DNA (ct-DNA) and 0.33 μM EB (saturated binding levels (Barton et al. 1986)) in 50 mM Tris–HCl at pH 7.4 buffer was titrated with aliquots of a concentrated solution of complex **1**, thus producing solutions with varied molar ratios of **1** to ct-DNA. After each addition the solution was stirred at the appropriate temperature during 5 min before measurement. The fluorescence spectra of the solution were obtained by exciting at 520 nm and measuring the emission spectra at the 530–700 nm range, using 5 nm slits. The procedure was the same for the Hoechst 33258 reactions, using the following conditions: working solutions were 20 μM ct-DNA and 2 μM Hoechst 33258; $\lambda_{ex} = 338$ nm and $\lambda_{em} =$ 400–550 nm (with $\lambda_{max} = 464$ nm).

Cathepsin B inhibition assay

Crude bovine spleen cathepsin B (cat B) was purchased from Sigma and used without further purification. The colorimetric cat B assay was performed in a solution containing 20 mM sodium acetate, and 1 mM EDTA at pH 5.1, using Z-L-Lys-ONp hydrochloride (Sigma) as the chromogenic substrate. In order for the enzyme to be catalytically functional, the cysteine residue present in the active site needs to be in a reduced form. Therefore, before using it, cat B was pre-reduced with dithiothreitol (DTT) to ensure that the majority of the enzyme is in a catalytically active form.

IC_{50} determinations were performed in duplicate using a fixed enzyme concentration of 0.1 μM, and a fixed substrate concentration of 0.1 mM. Inhibitor concentrations ranged from 0.25 to 75 μM. The enzyme and inhibitor were co-incubated at 25 °C over a period of 24 h prior to the addition of substrate. Activity was measured over 1 min at 327 nm.

Cysteine reactivation was evaluated using an inhibitor concentration corresponding to $2 \times IC_{50}$. The enzyme was treated with an excess of DTT (Sigma D0632). After the activation, the enzyme and compound **1** were incubated at 25 °C for 24 h. Then, 1 mM L-cysteine was added and incubated at different times 1, 2, 3, 4, 6 and 24 h at 25 °C. Following incubation, the substrate was added and activity was assessed.

Molecular modeling calculations

Quantum Mechanical (QM) optimizations have been performed on complex **1** and on several derivatives resulting from the substitution of the dmso or the azaindolate ligands with distinct models of amino acids. Calculations have been carried out with Gaussian 09 (2009) at the density functional theory (DFT) level using the B3LYP (Becke 1993; Lee et al. 1988); functional. The basis set used account for the 6–31 + G* (Hehre et al. 1972; Hariharan and Pople 1973; Spitznagel et al. 1982; Clark et al. 1983) for the main group elements and LANL2DZ (Hay and Wadt 1985) for Pt. LANL2DZ pseudopotential was also applied to the metal.

The strength of the interaction between the metal and its ligands has been evaluated using the energy decomposition analysis (EDA) as implemented in the ADF 2010 package (te Velde et al. 2001; Guerra et al. 1998; ADF 2010). Here, also calculations at DFT level have been performed with the becke (Becke 1988) and pw91c (Perdew et al. 1992) (for the correlation and exchange terms respectively) mixed functional. The basis set used in this part of the theoretical work was a TZP with a small frozen core for all the atoms, and ZORA formalism (van Lenthe et al. 1999) for the relativistic effects of the platinum centre.

Results and discussion

The previous characterization of the platinum(II) complex **1** showed its activity in several tumoral cell lines as well as modifications in the secondary structure of DNA (Ruiz et al. 2010), but no further data were reported regarding this interaction. To advance in the identification of the species formed in the process, the number of Pt atoms attached to distinct proteins to which complex **1** could bind before reaching its target, and the nature of its possible interactions with proteins and DNA were investigated.

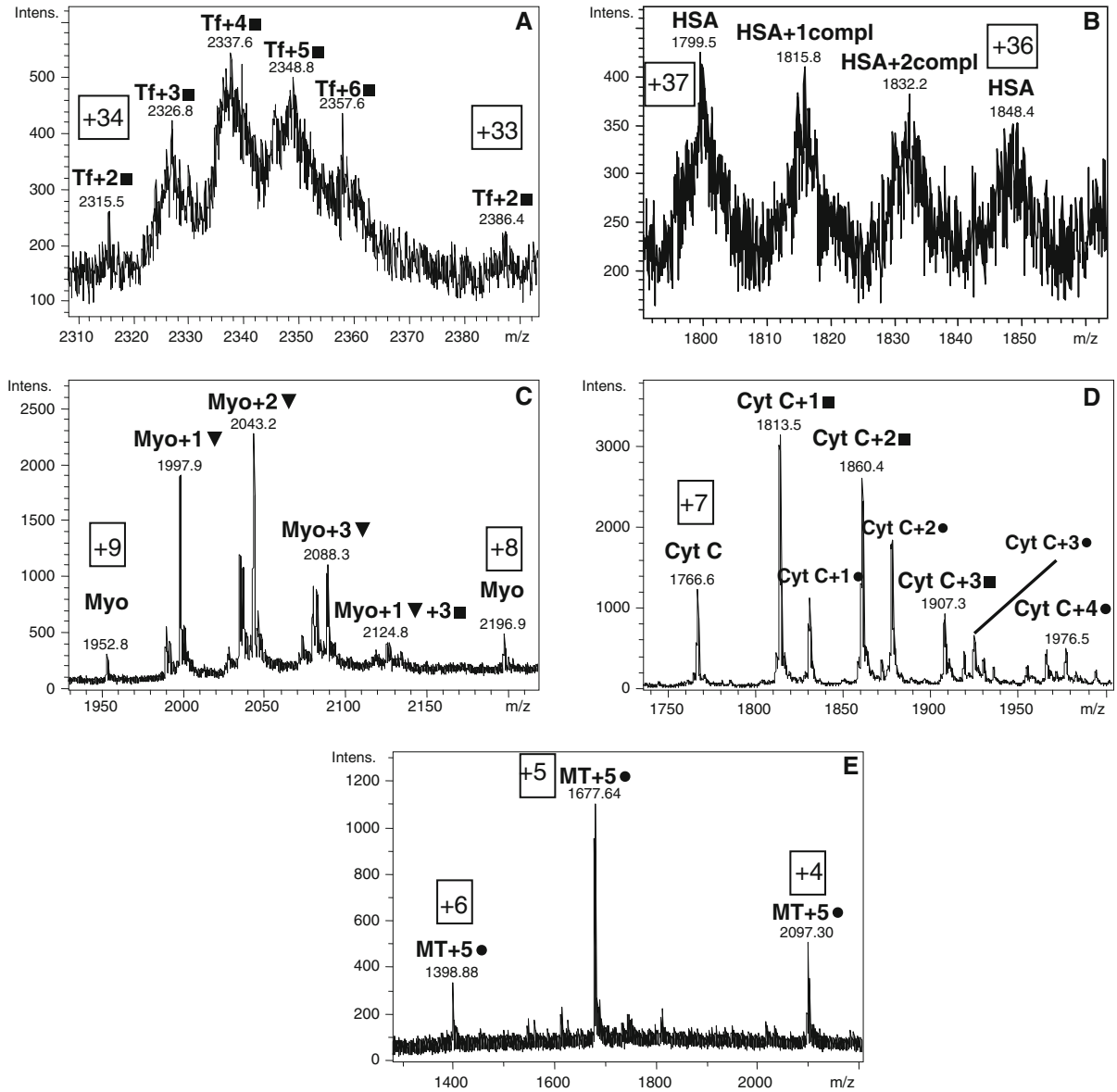

Fig. 2 Mass spectra recorded after incubation (24 h at 37 °C) of complex **1** with **a** transferrin (Tf), **b** albumin (HSA), **c** myoglobin (Myo), **d** cytochrome C (Cyt C) and **e** mammalian MT1 at a 1:10 (Protein:Pt) molar ratios. The numbers preceded by the "+" symbol in the boxes denote the charge state of the peaks. The notation "*n* compl" denotes a mass increase corresponding to the addition of "*n*" whole complexes **1** (524.5 mass units at the corresponding charge state) to the protein. The notation "*n*▼" indicates a mass increase corresponding to the addition of "*n*" molecules of complex **1** to the protein after the elimination of the initially bound azaindolate ligand ($C_7H_5N_2$) (524.5–117.1 mass units at the corresponding charge state); the notation "*n*●" indicates a mass increase corresponding to the addition of "*n*" molecules of complex **1** after elimination of the initially bound dmso (524.5–78.1 mass units at the corresponding charge state); and the notation "*n*■" indicates a mass increase corresponding to the addition of "*n*" molecules of complex **1** after elimination of both initial ligands, azaindolate and dmso (524.5–195.2 mass units at the corresponding charge state)

Moreover, the capabilities of the complex to inhibit cathepsin B have also been determined in order to check its possible role in the control of tumor progression.

Characterization of the proteins by ESI–MS

The proteins used in this work were previously analyzed by ESI-TOF MS in our labs by following a

reported procedure (Samper et al. 2012) in order to determine their experimental molecular weight under our working conditions (**Table S1**). The analysis of each protein solution lead to the observation of several ionization states in the described m/z working range, allowing a very precise determination of each individual MW. The spectra recorded for most of the protein preparations showed single species, except for albumin and transferrin, which exhibited several peaks, frequently associated to acetylated or distinct glycosylated forms (Castillo-Busto et al. 2009). The experimental MW recorded for myoglobin (17567 Da), 615 Da higher than that expected for the apoprotein, confirms the presence of the haem group (616.45 Da).

Interaction of the platinum(II) complex with the proteins

Complex **1** was incubated, at several molar ratios, with each of the chosen proteins (Tf, Myo, Cyt C, HSA and MT1). The whole set of mass spectra obtained allows to state that, despite complex **1** is able to react with all the assayed proteins, it does not show the same reactivity with all of them. For the sake of clarity, Table S2 contains all the information obtained (the species formed after the interaction with each protein and the relative intensity of their mass peaks), while Fig. 2 only shows the mass spectra recorded after incubation of **1** at the 1:10 protein-to-Pt molar ratios.

The ESI–MS data reveal that the species formed depend on two main factors: the nature of the protein and the assayed protein:Pt ratio. In the case of transferrin and albumin, a high amount of broad peaks, in low resolution spectra, were obtained (Figs. 2a, b respectively). However, within some experimental error, the corresponding species could be identified. Therefore, we can state that interaction of transferrin with **1** takes place through the elimination of both ligands, dmso and azaindolate (as deduced by the increase of multiples of 335 $\pm$ 7 mass units, *i.e.* Tf + n (compl-aza-dmso), *cf.* Fig 2 caption), from the coordination sphere of platinum (Fig. 2a). This is consistent with the observation that the composition of the distinct species was strongly dependent on the assayed protein-to-Pt ratios, being 6 the maximum of Pt moieties simultaneously attached to a single protein. Interestingly, no presence of the initial free transferrin was detected.

Very different are the results obtained with albumin, where the presence of peaks corresponding to the intact protein as the major species (Fig. 2b) denotes a poor interaction with **1**. The mass of the other observed peaks corresponds to the increase of multiples of ca. 550 $\pm$ 25 Da, suggesting that the Pt complex remains unaltered after protein binding, with a maximum ratio of two complexes per albumin molecule.

When the Pt complex **1** interacts with myoglobin (Fig. 2c) the main peaks observed inform about the binding of complex **1** after elimination of the azaindolate ligand (i.e. releasing of the ligand from the complex), although other minor peaks corresponding to the simultaneous release of both (aza + dmso) ligands were also observed (see **Table S2** for details). Oppositely, when **1** interacts with cytochrome C, the major peaks suggest the simultaneous elimination the azaindolate and the dmso ligands (i.e. releasing of both ligands), although minor peaks indicate the solely displacement of the dmso ligand (Fig. 2d).

Contrasting with literature data on the interaction of cisplatin with mammalian metallothioneins (Karotki et al. 2008), the incubation of **1** with the Zn-loaded form of MT1 rendered mainly the unreacted Zn_7-MT1 initial complex, together with very minor Zn_xPt_y-MT1 and Pt_5-MT1 species at the lowest Protein:Pt ratio assayed (**Table S2**). The partial or total substitution of the initially coordinated Zn^{2+} ions can be understood either considering the presence of small amounts of impurities accompanying complex **1** or Pt-binding mechanisms similar to those reported in the literature where all ligands of cisplatin are displaced (Karotki and Vasak 2008). Interestingly, at Pt-to-protein molar ratios higher than 1:1, the main detected peak shows the formation of a species containing 5 Pt complexes in which **1** only releases the dmso ligand (Fig. 2e).

Thus, overall data led to the observation that complex **1** can interact with the assayed proteins in three different ways: (a) through elimination of the azaindolate group (probably due to the *trans* effect of the C–Pt bond); (b) through elimination of the dmso molecule, mainly behaving as a monofunctional complex in both cases; and (c) by release of both ligands from the Pt coordination sphere, thus probably behaving as a bifunctional complex. Interestingly, the elimination of the ligand when binding to a certain protein seems to depend on the precise nature of the protein. Thus, the binding of the platinum moiety to

proteins apparently presents wider molecular patterns than expected.

In order to understand the basis of this differential reactivity, we took into consideration the amino acid sequences of the studied proteins, especially focusing on the presence of His and Cys, both amino acids normally associated to the coordination of Pt^{II} ions in biomolecules (Ivanov et al. 1998). Myoglobin contains 154 amino acids (11 His and 0 Cys), with some of the His residues easily accessible on its surface (as shown by the corresponding 3D structure, ref *3rgk* in the Protein Data Bank). Contrarily, MT1 has 62 amino acids, among them 20 Cys and 0 His. On the one hand, it can be considered that the interaction of complex **1** with myoglobin, probably binding by an N-donor atom of a His residue, causes the removal of the azaindolate ligand initially bound to the Pt(II) through one of its N atoms. On the other hand, it can be assumed that when **1** interacts with MT1, it binds to the Cys amino acids through their S atoms, so that the elimination of the dmso is compulsory to allow this interaction. Hence, it appears that the kind of interaction of complex **1** with proteins is directly related to the type of amino acid side chains available as ligand groups on the protein surface, *i.e.* N-donor or S-donor residues. This assumption correlates well with the observed reactivity of **1** with cytochrome C (3 His and 2 Cys over 105 total aa) and transferrin (22 His, 30 Cys, 622 total amino acid content), where the release of the azaindolate and the dmso ligands at the same time was observed, this indicating the participation of both types of residues of the proteins as ligands.

Another interesting conclusion can be drawn when analyzing the number of Pt atoms that result bound to each protein at the different molar ratios assayed. When comparing the species formed at the 1:10 molar ratio, Fig. 2, it becomes evident that: (a) transferrin can bind up to 6 Pt atoms; (b) myoglobin can bind up to 4 Pt, although the major species detected binds only 1 Pt complex; (c) cytochrome C shows binding of up to 4 Pt, but the main species contain only 1 Pt; and (d) albumin showed the interaction with up to 2 Pt complexes. If assuming that under our working conditions (close to those of physiological environments), all the proteins maintain its functional folding, the low number of Pt bound observed (in comparison with the high number of putative coordination sites available in the proteins) suggests that the groups interacting with the Pt centre need to be easily accessible, presumably on the surface of the protein, as already mentioned for myoglobin. The 3D structures available in the respective *3rgk* Protein Data Bank entry fully support this hypothesis. Hence, the myoglobin fold places only 3 His, among 11, close to the protein surface, while cytochrome C shows all their His and Cys as solvent-exposed residues. In the case of transferrin, its considerable size and its high number of putative ligands complicate the assignment of availability of its amino acid side chains. The case of albumin must be considered apart from the rest of proteins. Albumin is a huge protein, which also contains an elevated number of His and Cys residues, and which is devoted to the systemic transport of several types of metabolites (small molecules, metal ions, peptides, etc.). In fact, the mass peaks registered when **1** reacts with albumin can be related to the formation of adducts with the intact Pt complex, this suggesting that the inclusion of complex **1** in any of the existing cavities of the albumin globular structure is more likely than the formation of covalent bonds, contrarily to what probably happens with the rest of the assayed proteins.

Altogether, we can consider that the interaction of the Pt complex **1** with the proteins, except for MT1, may not alter significantly their structure if the Pt moiety ends bound to their surface or enclosed into the special cavities available for transportation, and consequently, proteins will keep all or part of their functionality. However, the interaction of **1** with MT1 deserves a special consideration, as it has provided significant unique results. The formation of a single species containing 5 Pt complexes bound per MT (where the dmso ligands have been released from the complex) suggests an especial type of interaction, probably due to a strong interaction of the Pt centre with the Cys residues of MT1. In order to better understand the interaction of **1** with the functional form Zn_7-MT1, we have monitored their reaction by optical spectroscopy (UV–vis absorption and circular dichroism, CD). Thus, to confirm that the single species observed, $[Pt(dmba)(aza\text{-}N1)]_5$-MT1, corresponds to an especially favoured aggregate only depending on the amount of **1** added to the protein, and to discard the possibility of an artefact formed when adding large quantities of **1**, two further experiments have been carried out. In the first one, aliquots of the solution of **1** were consecutively added to a 10 μM solution of Zn_7-MT1 in such a way that 1, 3

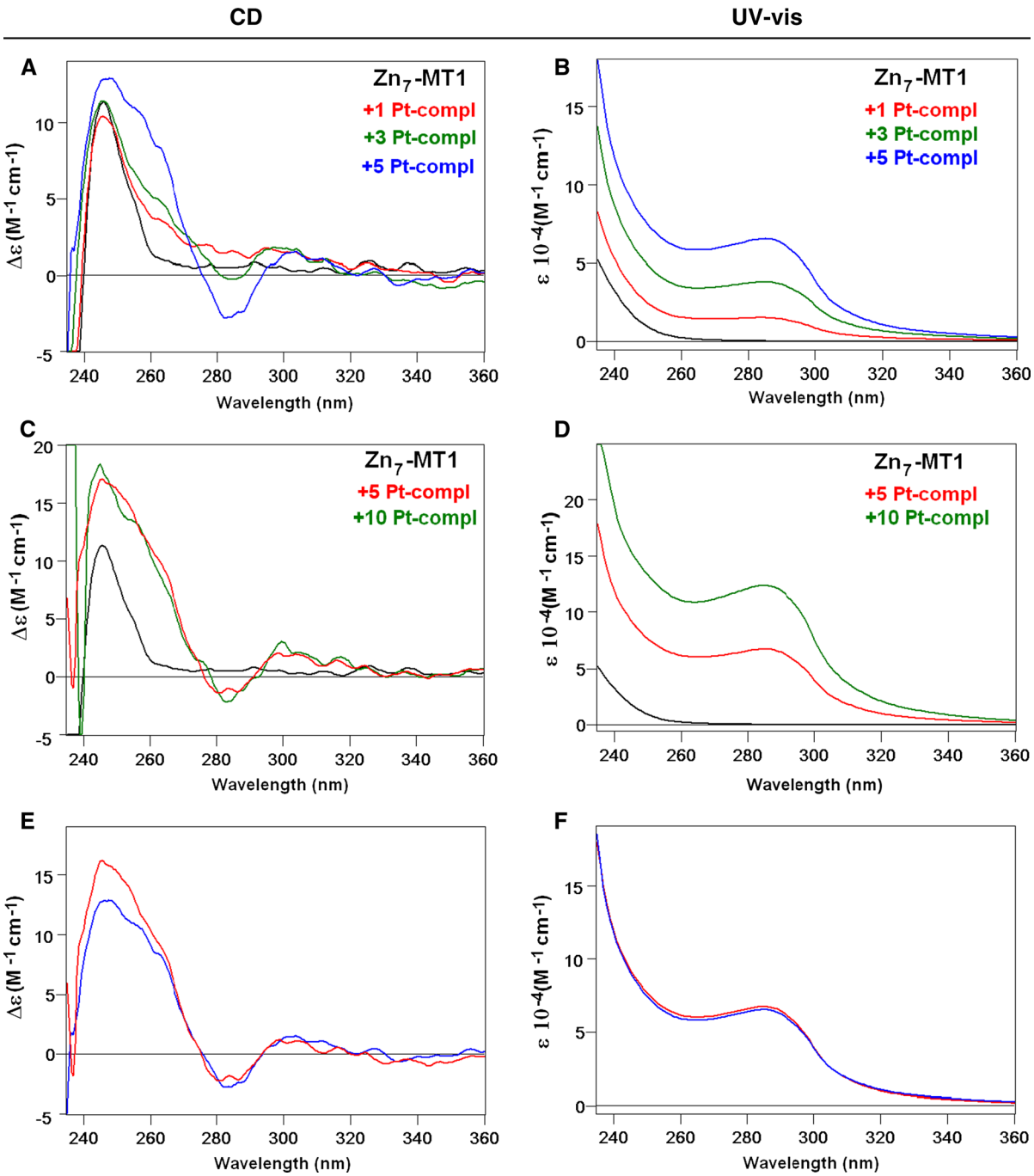

Fig. 3 Optical spectra recorded after the reaction of a 10 μM solution of Zn_7-MT1 with **a**, **b** 1, 3 and 5, and **c**, **d** 5 and 10 molar equivalents of **1**. Comparison of **e** the CD and **f** UV–vis spectra corresponding to the addition of 5 molar equivalents of **1** in both experiments (in *blue* as a result of the successive additions of 1, 3 and 5 molar equivalents of **1** and in red after adding 5 molar equivalents of **1** at once). All spectra were recorded after the incubation (1 h at 40 °C) of the samples

and 5 molar equivalents of **1** were coexisting with the protein at each step of the assay. In the second experiment, a similar approach was undertaken to have 5 and 10 molar equivalents of **1** added to a 10 μM solution of Zn_7-MT1. After each addition of the complex, the samples were incubated (1 h at 40 °C)

before registering the optical and the mass spectra of the resulting solution.

Addition of complex **1** to the Zn_7-MT1 solution implies the formation of new absorptions at ca. 290 nm (precisely an exciton coupling band in the CD spectra and a wide absorption band in the UV–vis spectra, Fig. 3) that can be associated to the binding of Pt to the protein. Interestingly, the spectra recorded after the addition of 5 molar equivalents of **1** in the two experiments, render practically identical spectra (Fig. 3e, f), which suggests that the species formed in both assays lead to a similar folding of the protein about the metal centre. The mass spectra recorded at each stage of each experiment (data not shown) yields identical information to that previously obtained (Fig. 2e and Table S2) and mass data collected after adding 5 molar equivalents of 1 in both assays are also practically coincident. Concluding, all our data reinforces the hypothesis that the species containing 5 Pt complexes bound to MT1, which is formed after releasing the initially-coordinated Zn^{2+} ions, results especially favoured in structure and energy terms.

When searching analogous complexes in the literature, it is interesting to highlight that **1** is the unique monomeric Pt-azaindolate complex reported. This group recently reported the reactivity of a similar Pt^{II}-dmba complex (Samper et al. 2012), where triphenylphosphine and aminoacridine were additional ligands. While the results here presented show that complex **1** interacts with almost all the assayed proteins, it should be taken into account that the previously reported Pt^{II}-dmba complex (Samper et al. 2012) exhibited a poor interaction with the same proteins, and that the reactivity of **1** is significantly lower than that reported for other Pt-based complexes (Casini et al. 2007), –and especially than those containing labile chloride ligands (Esteban-Fernández et al. 2010)- hence highlighting the importance of the whole set of ligands in the reactivity of these platinum complexes.

Theoretical calculations

The Pt complex, **1**, used in this work was specially designed with a dmso molecule bound to the platinum centre with the aim of facilitating its interaction with other molecules by releasing this ligand from the complex. Interestingly, experimental evidences show that **1** interacts with proteins in a different way than expected. Molecular Modeling was carried out to shed light on the origin of such behaviour focusing, in a first hypothesis, on pure bond energies.

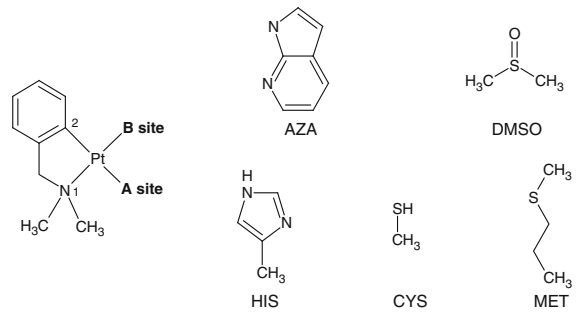

Fig. 4 Two dimensional representations of the fragments used to model the binding energies at each binding site. The two fixed binding atoms of the chelate ligand are denoted as N1 and C2. The original ligands present in complex **1** are the azaindolate (AZA) and the dimethylsulfoxide (DMSO) molecules. The models employed to simulate the coordinating amino acids are: 1-ethylimidazole as histidine (HIS); methylmercaptan as cysteine (CYS); and propylmethylthiol as methionine (MET)

DFT calculations with the B3LYP functional were undertaken on compound **1** as well as on all the complexes resulting from the ligand substitution at the azaindolate site (site A) or the dmso site (site B) by models of protein amino acids (Fig. 4). Amino acids considered in this study are the most commonly accepted platinum binding residues and correspond to histidine (modelled by 1-ethylimidazole), cysteine (modelled by a methylmercaptan) and methionine (modelled by a propylmethylthiol). For His and Cys, coordination has been considered for a neutral and negatively charged residue. Calculations were also undertaken with platinum bound throughout N_ε or N_δ atoms of the imidazole ring. Each system has been optimized with the Gaussian 09 package of program (Gaussian et al. 2009) with an extended basis set (see Experimental Section). In order to discuss the relative binding energies of the different residues to compound **1**, Energy Decomposition Analysis (EDA) as implemented in the ADF package (te Velde et al. 2001; Guerra et al. 1998; ADF 2010) has been carried out.

The optimized geometries of the different systems present square planar configurations about the metal centre, with little deviations from the ideality (Table S3 in Supplementary material). For sulfur containing residues, a slight distortion is observed with a dihedral angle, which is defined by the four coordinating atoms (B_{site}-A_{site}-N_1-C_2) directly connected to the platinum centre, of about 10°. Independently of the charge of the

ligand, Pt–S bonds exhibit the longest length observed (about 2.4 Å for methionine and cysteine, against the 2.2 Å for other coordinating groups, including dmso), thus suggesting weaker interactions of such species with the platinum moiety. Predicted binding energies of the dmso and the azaindolate ligands are estimated to −41.74 and −130.72 kcal mol^{-1}, respectively. Energetic breakdowns show that these differences mainly arise from electrostatic and steric contributions; something consistent with the anionic character and larger size displayed by the latter. However, this also suggests a weaker release of the azaindolate with respect to dmso; a result apparently inconsistent with the experimental evidences described above.

Detailed analysis of possible ligand exchange between amino acids and the compound **1** (Table 2) have been further analyzed by comparing their interaction energy with the metallic system. Substitutions at the dmso site (B) by residue fragments lead to stronger binding energies than for dmso and range from approximately 6 (for neutral residues) to 35 kcal mol^{-1} (for negatively charged residues). Interestingly, independently of the charge of the system, cysteine is always predicted as the best ligand for dmso substitution with about 1 to 6 kcal mol^{-1} higher predicted affinity than histidine. Moreover, intermediate situations with a water exchange prior to residue binding are unlikely because of the weak binding of water at the B site (−23.52 kcal mol^{-1}). Substitutions at the azaindolate site (A) lead to a wider spectrum of binding energies. For neutral residues, sulfur containing chelates bind at about −27 kcal mol^{-1}; a result in the same range of values than for water (−21 kcal mol^{-1}) while histidine has a slightly better interaction energy of approximately −40 kcal mol^{-1}. None of them would be predicted to exchange with the original ligand in its anionic nature because of the large difference in energy to overcome (about 100 kcal mol^{-1}). For anionic species, predicted binding energies are in the same range, or even higher, than for the azaindolate. In particular, coordination of the cysteinate is close to 144 kcal mol^{-1} (14 kcal mol^{-1} stronger than the azaindolate) and coordination of the histidinate through the δ nitrogen is about −195 kcal mol^{-1} (65 kcal mol^{-1} less than the azaindolate). This shows that substitution at the A site could take place with the standard platinum binding residues with a preference, again, for histidine.

At this point, the rationalization of the substitutions experimentally observed at site A can only be obtained by considering a negatively charged His^{-} (N_δ) exchange with the azaindolate ligand. This suggests that the protonation state of the azaindolate could have a weight into the binding process. Therefore, an additional calculation has been performed for which the azaindolate has been protonated, a situation possible considering the pKa values of the ligand. Such modification of the nature of the ligand leads to an energy of interaction of −23.27 kcal mol^{-1}. In this case, site A becomes far more labile than site B as the resulting binding energy shows that substitution by any residue can occur. Interestingly, such substitution should take place primarily with histidine. Although the dynamical considerations and the full mechanism of exchange between histidine and azaindolate are not taken into account at this point, our calculations clearly point at the importance of changes in the nature of the protonation state of the ligands to understand the experimental observations. However, more calculations are needed to be carried out to confirm the proposed mechanism.

Table 2 Main energetic contributions, steric and orbital, as well as total interaction energy, of different ligands at the A and B sites of complex **1**

Ligand	Interactions (kcal mol^{-1})		Total bonding energy (kcal mol^{-1})
	Steric	Orbital	
Site A			
AZA	−58.39	−72.32	−130.72
CYS	15.37	−41.01	−25.64
HIS (N_ε)	4.61	−45.76	−41.15
HIS (N_δ)	7.34	−45.77	−38.42
MET	13.89	−42.07	−28.17
H_2O	9.52	−30.89	−21.37
AZA + H	13.04	−36.31	−23.27
CYS^-	−60.14	−84.29	−144.43
HIS^- (N_ε)	−53.36	−74.88	−128.24
HIS^- (N_δ)	19.79	−215.1	−195.31
Site B			
dmso	31.68	−73.42	−41.74
CYS	23.31	−71.38	−48.07
HIS (N_ε)	17.82	−64.91	−47.09
HIS (N_δ)	19.37	−67.12	−47.75
MET	23.03	−69.06	−46.03
H_2O	13.42	−36.95	−23.52
CYS^-	15.76	−99.58	−83.81
HIS^- (N_ε)	12.76	−87.97	−75.21
HIS^- (N_δ)	13.76	−88.07	−74.66

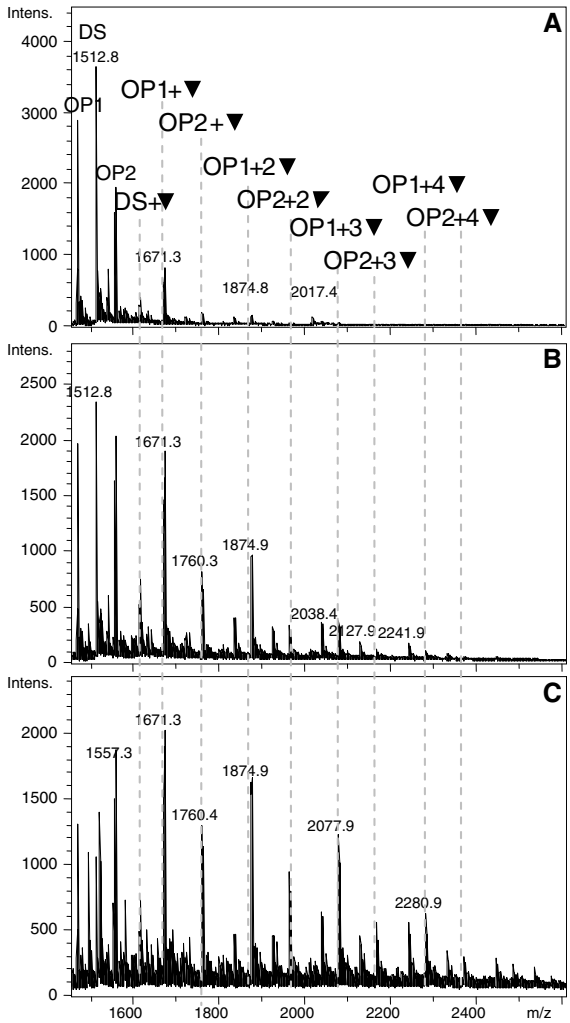

Fig. 5 Negative ESI-TOF MS spectra obtained after incubation (24 h at 37 °C) of mixtures of the double-stranded chain (DS) with increasing amounts of complex **1** at **a** 1:1, **b** 1:5 and **c** 1:10 DS:Pt molar ratios. The notation "*n*▼" indicates a mass increase corresponding to the addition of "*n*" molecules of complex **1** after the elimination of its initial azaindolate ligand ($C_7H_5N_2$). (117.1 mass units at the shown charge state, which is m/z = 58.6). Other minor non-labelled peaks correlate with species formed between 1 and the oligonucleotides after elimination of both ligands, the azaindolate and the dmso

Interaction of the platinum(II) complex with oligonucleotides

The oligonucleotides used in this work were designed as single stranded (SS) and double stranded (DS) Pt-binding probes. After preparation of the DS by mixing the OP1 and OP2 SS oligonucleotides under optimal experimental conditions (see *Experimental section*), this solution was incubated at 37 °C with **1** at different molar ratios (DS:Pt ratios of 1:1, 1:5, and 1:10) during ca. 24 h and was analyzed by ESI–MS spectrometry.

The results obtained (Fig. 5) show the presence of several MS peaks mainly attributable to the binding of **1** (after release of the azaindolate ligand) to the single stranded oligonucleotides. The number of peaks, and thus of different species, significantly increases with the increase of the Pt:oligonucleotide ratio, while concomitantly decreases the intensity of the DS peak. Even though the stoichiometry of the species formed (*i. e.* the number of Pt atoms bound to each oligonucleotide) directly depends on the amount of complex **1** added, at the 1:5 and 1:10 molar ratios the major peaks observed correspond to the binding of only one Pt complex to each SS oligonucleotide (OP1 + ▼; OP2 + ▼).

Other minor peaks were detected in the mass spectra: on the one hand, a single peak associated to the direct binding of **1** to the DS after the release of the azaindolate ligand (denoted as DS + ▼, with m/z = 1614.3); and on the other hand, small peaks that correlate with binding of the Pt complex **1** to the single stranded oligonucleotides after elimination of both the azaindolate and the dmso ligands, specially observed at the highest Pt:protein ratio assayed. Taking into consideration the previously studied (vide supra) reactivity of **1** with proteins, these results suggest that Pt^{II} preferentially binds to an N-donor ligand present in the oligonucleotides, presumably their nitrogenous bases. Several attempts to determine the binding sites of the Pt-moiety were carried on by MS/MS experiments at different Pt:DS molar ratios but no results suggesting a preferential binding of **1** to any specific single strand or nucleotide were obtained (data not shown).

The results here presented also indicate that most of the observed peaks correlate with the binding of **1** to a single oligonucleotide (OP1 or OP2) rather than to DS as only one DS + ▼ peak was identified. This can be explained through two different hypotheses: (i) one possibility is that the final scenario corresponds to the interaction of complex **1** with the single stranded molecules that remain in the solution after a partial annealing process, and (ii) another possibility relies in considering that the dramatic loss of intensity of the original DS peak when increasing the Pt:oligonucleotide ratio, but not of those of OP1 and OP2, may indicate that the interaction of **1** with the double-

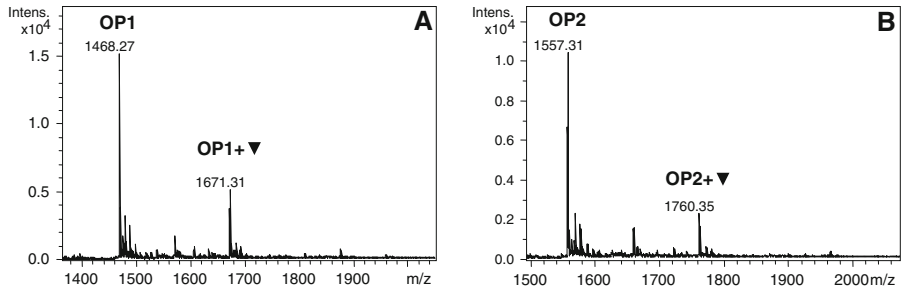

Fig. 6 Negative ESI-TOF MS spectra recorded after incubation (24 h at 37 °C) of complex **1** with the individual oligonucleotides **a** OP1 and **b** OP2, at a 1:10 oligonucleotide:Pt ratio, showing a charge state of −2 for all the peaks. The notation "▼" indicates a mass increase corresponding to the addition of one molecule of **1** after the elimination of its initial azaindolate ligand ($C_7H_5N_2$). (117.1 mass units at the corresponding charge state)

stranded molecule promotes its melting into the single-stranded oligonucleotides. In order to test these two possibilities, two further experiments were designed. First, each of the single stranded oligonucleotides, OP1 and OP2, was incubated at a 1:10 oligonucleotide:Pt ratio. As a result, only minor peaks suggestive of Pt-binding were observed in both cases (Fig. 6), a situation quite far away from the more intense peaks of the same species observed in the previous experiment at the same Pt:oligonucleotide ratio (Fig. 5c).

Secondly, the annealed DS form was separated by size exclusion-HPLC of the remaining SS oligonucleotides before incubation of the former with complex 1. The purification of DS was successfully achieved due to the different retention times of the single- and double-stranded oligonucleotides (Fig. 7a). The DS thus purified (Fig. 7b) was incubated with 1 at different molar ratios (Fig. 7c–f) and the mixtures analyzed by ESI–MS. The recorded mass spectra show a drastic decrease of the relative intensity of the peak corresponding to the free DS form with the increasing amounts of **1**, while the relative intensity of the peaks of OP1 and OP2 slightly increased. The absence of MS peaks at m/z higher than 1,600, *i.e.* those corresponding to the Pt-derivatives already observed in the previous experiments, can be explained if we consider that the concentration of the eluate resulting from chromatography was estimated to be lower than 5 μM, which clearly impairs the observation by mass spectrometry of several coexisting species. Interestingly, the same experiment carried out in the absence of **1**, *i. e.* incubation of the DS and further chromatographic purification, show that the intensities of DS and SS remained unaltered, recording the same mass spectra as that in Fig. 7b.

The results of these two last experiments (Figs. 6, 7) confirm the second initial hypothesis: the Pt complex 1 reacts almost exclusively with the DS and, due to this interaction, the double helix melts into the SS oligonucleotides. This could be probably explained taking into account the small size of the double chain (only 10 bp), which is probably destabilized after Pt binding.

In order to confirm the interaction of **1** with DS, it was incubated (12 h at 37 °C) with **1** at the 1:1 and 1:5 DS:Pt ratios, and the corresponding CD spectra registered (Fig. 8). These show that the presence of complex **1** provokes a clean decrease of the intensity of the initial spectropolarimetric fingerprint of DS in the 290 nm region at the 1:5 DS:Pt ratio from the early stages of the reaction (1 min), and that was completed after 12 h. Interestingly, no modification of the secondary structure of DS was observed at the 1:1 DS:Pt ratio, which is indicative of the stability of the 10-bp DS fragment under the assayed conditions. These results suggests that the complex can cause modifications in the secondary structure of DNA at the appropriate DNA:Pt ratios.

The reactivity here observed for complex **1** with DS oligonucleotides clearly differs from that we recently reported for a similar Pt^{II}-dmba complex (Samper et al. 2012). The strong covalent interaction of **1** after release of the azaindolate ligand contrasts with the π interaction reported for the latter, which is due to the presence of an aminoacridine ligand. This confirms that in spite of the stabilizing role of the dmba chelating ligand in the structure of the complex, its reactivity can be tuned through the modulation of the nature of the two other ligands bound to the Pt^{II} moiety.

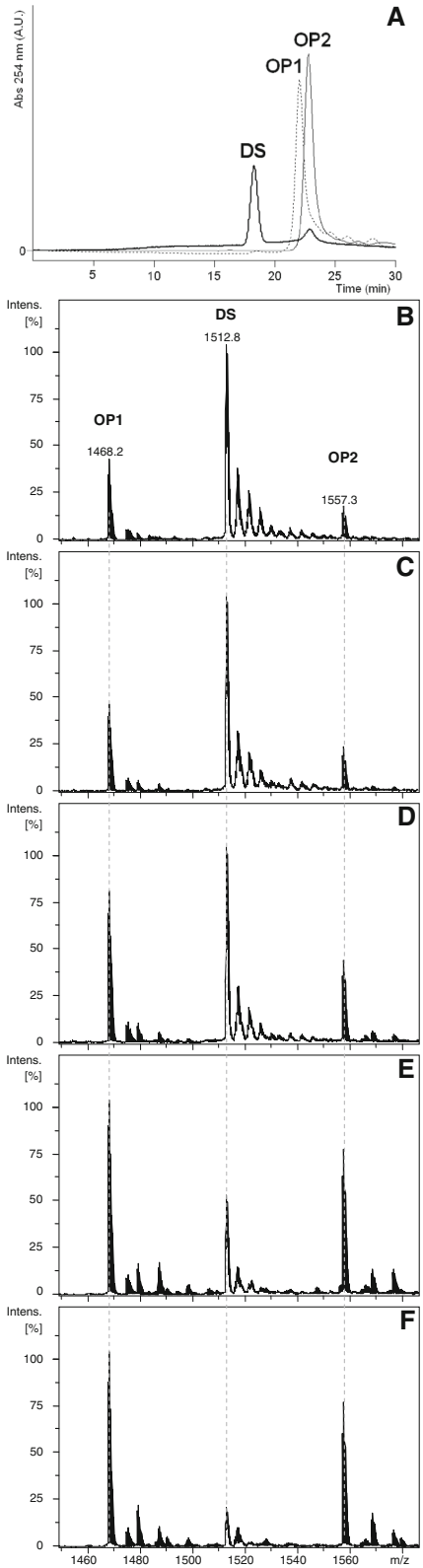

◀**Fig. 7** **a** Size exclusion HPLC chromatograms corresponding to the individual SS oligonucleotides, OP1 and OP2, and the profile obtained after their incubation (2 h at 70 °C) to form the double-stranded form (DS). Negative ESI-TOF MS spectra recorded **b** after separation of the DS fraction form the SS oligonucleotides, and after incubation of the DS fraction with **1** at the Pt:DS **c** 1:1, **d** 5:1, **e** 10:1, and **f** 20:1 molar ratios

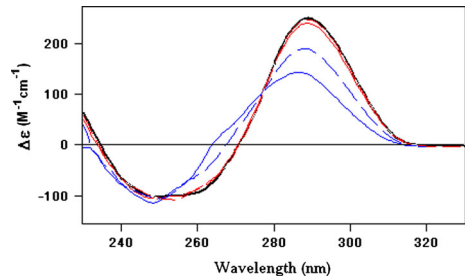

Fig. 8 CD spectra recorded after the incubation of a 5 μM solution of DS (*black line*) with 1 (*red*) and 5 (*blue*) molar equivalents of **1** registered after 1 min (*dashed*) and after 12 h (*solid*) of incubation at 37 °C

Competitive binding experiments

In order to further investigate the interaction between complex **1** and DNA, fluorescence competition experiments with ethidium bromide (EB) and Hoechst 33258 were carried out. EB is a planar cationic dye well-known to intercalate into the DNA double helix (Bresloff and Crothers 1975; Le Pecq 1971). While EB is only weakly fluorescent, the EB–DNA adduct is a strong emitter (near 620 nm) when excited near 520 nm. Quenching of the fluorescence may be used to determine the extent of the binding between the quencher **1** and commercial calf thymus DNA (ct-DNA). As seen in Fig. 9a, complex **1** can compete with EB for the DNA binding sites as there is a decrease in the fluorescence (by 28 % of the initial) at 602 nm with the increase of the amount of **1** added to the EB-DNA mixture. This suggests the idea that **1** could also interact with DNA by the intercalative mode, although the reason for the quenching of the EB-DNA adducts could also be the reduction in the number of available binding sites on DNA, presumably due to the competition with the complex, which is non-emissive under the experimental conditions (Beckford et al. 2011a, b; Ruiz et al. 2013).

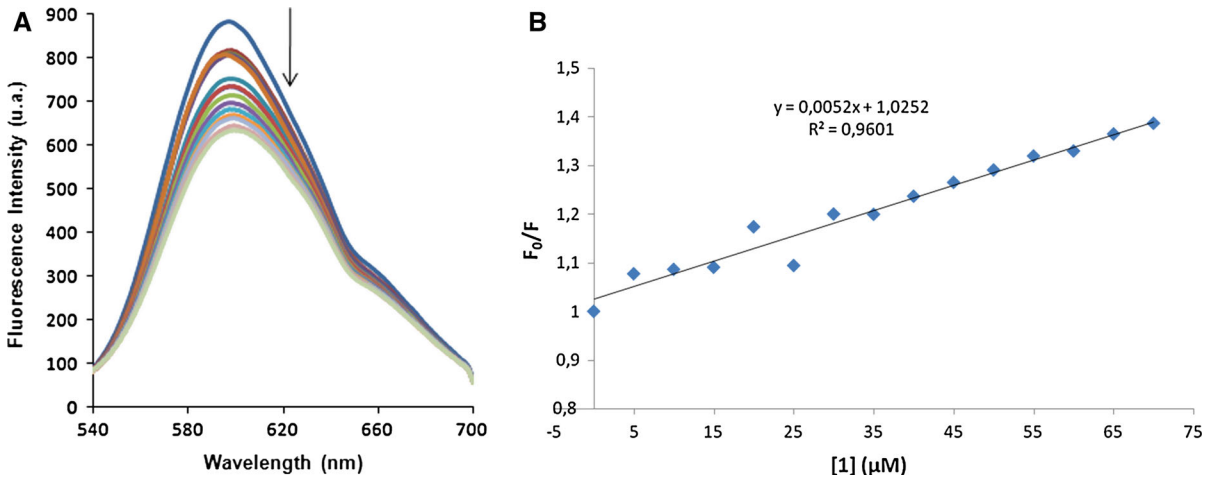

Fig. 9 **a** Fluorescence spectra of EB bound to ct-DNA (*solid blue line*) in aqueous buffer solution in the presence of increasing amounts of **1**, at 298 K. $\lambda_{ex} = 520$ nm, [EB] = 0.33 μM, [DNA] = 10 μM, [complex **1**] (μM): 0–70 in 5 μM increments. **b** Stern–Volmer plot with the results obtained for the titration of EB bound to ct-DNA with **1**

In order to quantitatively assess the magnitude of the interaction between complex **1** and ct–DNA, the Stern–Volmer equation is used: $F_0/F = 1 + K_{SV}[Q]$ where F and F_0 respectively are the fluorescence intensities of the DNA solution in the presence and absence of the complex, K_{SV} is the Stern–Volmer quenching constant and [Q] is the concentration of **1**. The good linearity of the Stern–Volmer plot (Fig. 9b) suggests a singular mode of quenching. The value of K_{SV} was 5.2×10^3 M^{-1}, which depicts complex **1** as a weak intercalator. The apparent binding constant (K_{app}) for the complex was 3.11×10^3 M^{-1}, calculated using the equation: $K_{app} = K_{EB}[EB]/[Q]_{50}$, where $K_{EB} = 1.2 \times 10^6$ M^{-1} (Peberdy et al. 2007). The K_{EB} value is the binding constant of EB to DNA and $[Q]_{50}$ is the concentration of **1** at 50 % of the initial fluorescence. One reason for the quenching of the EB-DNA adducts can be the already mentioned reduction in the number of available binding sites on DNA by competition with the complex.

Furthermore, we carried out another competition experiment using the Hoechst 33258 stain. This fluorescent dye binds to DNA and when this happens its fluorescence yield increases significantly (Weisblum and Haenssler 1974). Displacement by a competitor of the bound dye from its binding site leads to a decrease in the fluorescence intensity. It is well known that Hoechst 33258 binds to DNA in two concentration dependent ways, the first type of binding occurring in the minor groove at low dye-to-DNA ratios,

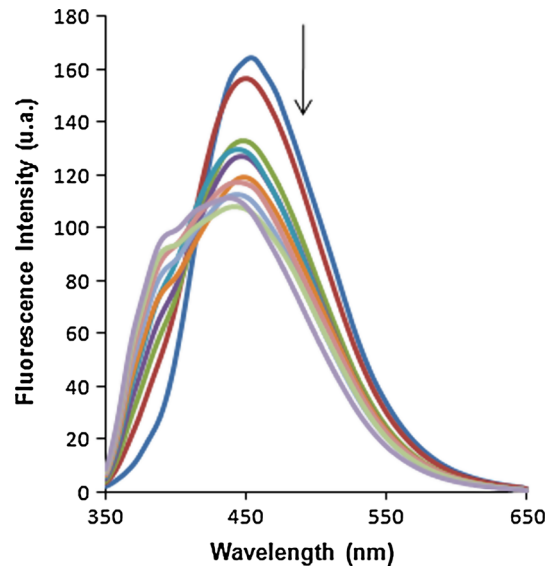

Fig. 10 Fluorescence spectra of the Hoechst 33258-bound ct-DNA in aqueous buffer solution, in the absence (*solid blue line*) and presence of increasing amounts of complex **1**, recorded at 298 K. $\lambda_{ex} = 338$ nm, [Hoechst 33258] = 2 μM, [ct-DNA] = 20 μM, [complex **1**] (μM): 0–15 in 2.5 μM increments and 15–30 in 5 μM increments

which are the conditions we have assayed (Pjura et al. 1987; Guan et al. 2007). When complex **1** was added to Hoechst-ct-DNA solution a decrease (~33 %) in the fluorescence and the appearance of one peak at about 396 nm was observed (Fig. 10). The first effect suggests that complex **1** is able to weakly bind ct-DNA

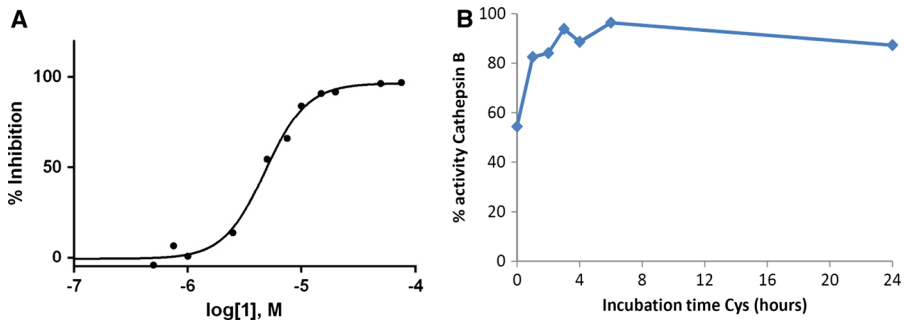

Fig. 11 **a** Cat B activity inhibition curve for complex **1**. **b** Cysteine reactivation of cat B inhibited by 2 × IC_{50} μM of **1**, in the presence of 1 mM cysteine. The first measurement was taken 5 min after the addition of cysteine

at the minor grove and the second was attributed to the fluorescence of the Pt(II) complex.

In vitro evaluation of the bovine cat B inhibitory activity of complex **1**

Cathepsin B (cat B) was proposed as a therapeutic target for the control of tumor progression (Strojnik et al. 1999) because the use of cat B inhibitors reduces both in vitro tumor cell mobility and invasiveness (Podgorski and Sloane 2003). Some metal complexes have been shown to be effective inhibitors of cat B (Casini et al. 2008). Hence, complex **1** was evaluated for activity against bovine cat B with an in vitro IC_{50} of 4.86 ± 0.02 μM (obtained from Fig. 11a, which illustrates the inhibition of enzyme activity provoked by the presence of **1**). These results indicate that **1** is a very good cathepsin B inhibitor.

Additionally, the reactivation of cat B (after the previous inhibition) by the presence of cysteine (Fig. 11b) was evaluated in order to characterize the reversibility of the inhibition promoted by **1**. It was found that the addition of 1 mM cysteine to the 0.1 μM cat B inhibited solution results in almost full recovery of activity within a few hours (more than 80 % of initial enzyme activity was already restored after 3 h). Overall, these data support the hypothesis that loss of enzyme activity is mainly due to the specific interaction of **1** with the cat B active site instead of an enzyme denaturing process induced by the presence of the platinum complex.

Conclusions

In this work, we propose that the reactivity of the (7-azaindolato-κN1)(*N*,*N*-dimethylbenzylamine-κN,κC)-(dimethylsulfoxide-κS)platinum(II) complex, **1**, with several proteins takes place, in most of the cases, by binding of compound **1** to the more accessible coordinating amino acids of the surface of the proteins. Consequently, this interaction would not lead to the subsequent protein denaturation or degradation. The specific reactivity of **1** with the chosen proteins allows to conclude that the Pt-ligand displaced in each case (dmso or azaindolate) is indicative of the nature of the protein ligand bound to the Pt^{II} centre. Thus, when the Pt^{II} moiety binds a S-atom of a Cys residue, the dmso is released from the complex, while the azaindolate is displaced when it binds to a N-atom of a His residue. The theoretical calculations here performed suggest that the release of the azaindolate ligand is promoted by a proton transfer to the non-coordinating N of the azaindolate ligand. Molecular modeling analysis of the interaction energies between common Pt-coordinating amino acids and complex **1** suggests that substitution at the initial azaindolate or dmso binding sites with histidines are a likely event. The experimental observation of a stronger interaction of the azaindolate than the dmso site with myoglobin is rationalized by assuming a change of the protonation state of the ligand at site A. This could result from a protonation of the azaindolate in solution or a deprotonation of the histidines of the protein. Although not reported yet for amino acids, this observation is consistent with the already reported huge shifts of pKa of biological building blocks in presence of metals (Lippert 2008; Roitzsch et al. 2005). Moreover, in both cases, such results consistently account for the importance of the *trans* effect in the substitution of cis-platinum derivatives (Montero et al. 2010; Manalastas et al. 2009). Further QM and QM/MM calculations on the entire mechanism of ligand substitutions and possible proton transfer occurring during such process would shed light on this aspect. The interaction of the Pt complex with the mammalian Zn_7-MT1 complex indicates the

formation of a single, unexpected species containing 5 Pt-complex units without the initial dmso ligand, with displacement of all the initial Zn^{2+} ions bound to the peptide. Furthermore, the formation of this particular species appears to depend only on the protein:complex ratio assayed.

The interaction of complex **1** with the OP1 and OP2 oligonucleotides show a strong covalent binding of the Pt^{II} centre to both of them, in a similar way -it is without a special preference for one or another-, and in all cases with release of the initial azaindolate ligand. Interestingly, this interaction seems to occur only when both oligonucleotides are annealed forming a double strand. Circular dichroism data corroborate the modification of the secondary structure of DS by the presence of complex **1**. Furthermore, competing experiments with ethidium bromide and Hoechst 33258 displacement show that **1** is able to weakly bind to ct-DNA, probably in the minor groove. Additionally, complex **1** has been shown to be a good cathepsin B inhibitor, most probably interacting with the active site of the enzyme.

Concluding, compound **1** should be taken into consideration as a putative anticancer drug due to its strong interaction with oligonucleotides and its effective inhibition of cathepsin B, although it is definitely able to bind proteins that can hamper its arrival to the nuclear target. Significantly, the specific reactivity of **1** when interacting with S- or N-donor ligands, owing to the presence of the azaindolate ligand, opens a new way to modulate and direct Pt^{II} binding to specific targets.

Acknowledgments This work was supported by the Spanish *Ministerio de Ciencia e Innovación* and FEDER through the following projects: SAF2011-26611 to J. Ruiz, BIO2012-39682-C02-01 to S. Atrian, and BIO2012-39682-C02-02 to M. Capdevila; CTQ2008-06866-C02-01 and consolider-ingenio 2010 to J.-D. Marechal. J. Ruiz also acknowledges the financial support received from *Fundación Seneca-CARM* (Project 08666/PI/08). The authors from UAB and UB are members of the *Grup de Recerca de la Generalitat de Catalunya* refs. 2009SGR-1457 and 2009SGR-68. S. Artime, at S. Atrian's lab, was responsible of the recombinant synthesis of Zn_7-MT1.

References

ADF (2010) SCM, Theoretical Chemostry, Vrije Universiteit, Amsterdam, The Netherlands, http://www.scm.com

Barnes KR, Lippard SJ (2004) Cisplatin and related anticancer drugs: recent advances and insights. Met Ions Biol Syst 42:143–147

Barton JK, Goldberg JM, Kumar CV, Turro NJ (1986) Binding modes and base specificity of tris(phenanthroline)ruthenium(II) enantiomers with nucleic acids: tuning the stereoselectivity. J Am Chem Soc 108(8):2081–2088

Becke AD (1988) Density-functional exchange-energy approximation with correct asymptotic behaviour. Phys Rev A 38(6):3098–3100

Becke AD (1993) Density-functional thermochemistry. III. The role of exact exchange. J Chem Phys 98:5648–5652

Beckford F, Dourth D, Shaloski M Jr, Didion J, Thessing J, Woods J, Crowell V, Gerasimchuck N, Gonzalez-Sarrías A, Seeram NP (2011a) Half-sandwich ruthenium-arene complexes with thiosemicarbazones: synthesis and biological evaluation of [(η6-p-cymene)Ru(piperonal thiosemicarbazones)Cl]Cl complexes. J Inorg Biochem 105(8):1019–1029

Beckford F, Thessing J, Woods J, Didion J, Gerasimchuck N, Gonzalez-Sarrías A, Seeram NP (2011b) Synthesis and structure of [(η6-p-cymene)Ru(2-anthracen-9-ylmethylene-N-ethylhydrazinecarbothioamide)Cl]Cl; biological evaluation, topoisomerase II inhibition and reaction with DNA and human serum albumin. Metallomics 3(5): 491–502

Bresloff JL, Crothers DM (1975) DNA-ethidium reaction kinetics. Demonstration of direct ligand transfer between DNA binding sites. J Mol Biol 95(1):103–123

Casini A, Gabbiani C, Mastrobuoni G, Pellicani RZ, Intini FP, Arnesano F, Natile G, Moneti G, Francese S, Messori L (2007) Insights into the molecular mechanisms of protein platination from a case study: the reaction of anticancer platinum(II) iminoethers with horse heart cytochrome C. Biochemistry 46(43):12220–12230

Casini A, Gabbiani C, Sorrentino F, Rigobello MP, Geldbach ABTJ, Marrone A, Re N, Hartinger CG, Dyson PJ, Messori L (2008) Emerging protein targets for anticancer metallodrugs: inhibition of thioredoxin reductase and cathepsin B by antitumor ruthenium(II)-arene compounds. J Med Chem 51(21):6773–6781

Castillo-Busto ME, Meija J, Montes-Bayón M, Sanz-Medel A (2009) Diophantine analysis complements electrospray-Q-TOF data for structure elucidation of transferrin glycoforms used for clinical diagnosis in human serum and cerebrospinal fluid. Proteomics 9(4):1109–1113

Clark T, Chandrasekhar J, Spitznagel GW, Schleyer PR (1983) Efficient diffuse function-augmented basis sets for anion calculations. III. The 3–21 + G basis set for first-row elements, lithium to fluorine. J Comput Chem 4(3): 294–301

Cols N, Romero-Isart N, Capdevila M, Oliva B, Gonzàlez-Duarte P, Gonzàlez-Duarte R, Atrian S (1997) Binding of excess cadmium(II) to Cd7-metallothionein from recombinant mouse Zn7-metallothionein 1. UV-VIS absorption and circular dichroism studies and theoretical location approach by surface accessibility analysis. J Inorg Biochem 68(3):157–166

Egger AE, Hartinger CG, Hamidane HB, Tsybin YO, Keppler BK, Dyson PJ (2008) High resolution mass spectrometry

for studying the interactions of cisplatin with oligonucleotides. Inorg Chem 47(22):10626–10633

Esteban-Fernández D, Moreno-Gordaliza E, Cañas B, Palacios MA, Gómez-Gómez MM (2010) Analytical methodologies for metallomics studies of antitumor Pt-containing drugs. Metallomics 2(1):19–38

Fernandez P, Farre X, Nadal A, Fernandez E, Peiro N, Sloane BF, Sih G, Chapman HA, Campo E, Cardesa A (2001) Expression of cathepsins B and S in the progression of prostate carcinoma. Int J Cancer 95(1):51–55

Gaussian 09, Frisch MJ, Trucks GW, Schlegel HB, Scuseria GE, Robb MA, Cheeseman JR, Scalmani G, Barone V, Mennucci B, Petersson GA, Nakatsuji H, Caricato M, Li X, Hratchian HP, Izmaylov AF, Bloino J, Zheng G, Sonnenberg JL, Hada M, Ehara M, Toyota K, Fukuda R, Hasegawa J, Ishida M, Nakajima T, Honda Y, Kitao O, Nakai H, Vreven T, Montgomery JA, Peralta Jr.JE, Ogliaro F, Bearpark M, Heyd JJ, Brothers E, Kudin KN, Staroverov VN, Kobayashi R, Normand J, Raghavachari K, Rendell A, Burant JC, Iyengar SS, Tomasi J, Cossi M, Rega N, Millam JM, Klene M, Knox JE, Cross JB, Bakken V, Adamo C, Jaramillo J, Gomperts R, Stratmann RE, Yazyev O, Austin AJ, Cammi R, Pomelli C, Ochterski JW, Martin RL, Morokuma K, Zakrzewski VG, Voth GA, Salvador P, Dannenberg JJ, Dapprich S, Daniels AD, Farkas Ö, Foresman JB, Ortiz JV, Cioslowski J, Fox DJ (2009) Gaussian, Inc., Wallingford CT

Guan Y, Shi R, Li X, Zhao M, Li Y (2007) Multiple binding modes for dicationic Hoechst 33258 to DNA. J Phys Chem B 111(25):7336–7344

Guerra CF, Snijders JG, te Velde G, Baerends EJ (1998) Towards an order-N DFT method. Theor Chem Acc 99(6):391–403

Hariharan PC, Pople JA (1973) Influence of polarization functions on MO hydrogenation energies. Theor Chim Acta 28(3): 213–222

Harper BW, Krause-Heuer AM, Grant MP, Manohar M, Garbutcheon-Singh KB, Aldrich-Wright JR (2010) Advances in Platinum Chemotherapeutics. Chem Eur J 16(24): 7064–7077

Hay J, Wadt WR (1985) Ab initio effective core potentials for molecular calculations. Potentials for potassium to gold including the outermost core orbitals. J Chem Phys 82(1):299–310

Hehre WJ, Dirchfield R, Pople JA (1972) Self-consistent molecular orbital methods. XII. Further extensions of gaussian-type basis sets for use in molecular orbital studies of organic molecules. J Chem Phys 56:2257–2261

Ivanov AI, Christodoulou J, Parkinson JA, Barnham KJ, Tucker A, Woodrow J, Sadler PJ (1998) Cisplatin binding sites on human albumin. J Biol Chem 273(24):14721–14730

Jakupec MA, Galanski M, Arion VB, Hartinger CG, Keppler BK (2008) Antitumor metal compounds: more than theme and variations. Dalton Trans 2:183–194

Jamieson ER, Lippard SJ (1999) Structure, recognition, and processing of cisplatin-DNA adducts. Chem Rev 99(9): 2467–2498

Karotki AV, Vasak M (2008) Interaction of Metallothionein-2 with Platinum-Modified 5′-Guanosine Monophosphate and DNA. Biochemistry 47(41):10961–10969

Knipp M, Karotki AV, Chesnov S, Natile G, Sadler PJ, Brabec V, Vasak M (2007) Reaction of Zn7Metallothionein with cis- and trans-[Pt(N-donor)2Cl2] anticancer complexes: trans-PtII complexes retain their N-donor ligands. J Med Chem 50(17):4075–4086

Le Pecq JB (1971) Use of ethidium bromide for separation and determination of nucleic acids of various conformational forms and measurement of their associated enzymes. Methods Biochem Anal 20:41–86

Lee C, Yang W, Parr RG (1988) Development of the Colle-Salvetti correlation-energy formula into a functional of the electron density. Phys Rev B 37(2):785–789

Lippert B (1999) Cisplatin: chemistry and biochemistry of a leading anticancer drug, 1st edn. Helvetia Chimica Acta/Wiley-VCH, Zurich/Weinheim, p 576

Lippert B (2008) Ligand-pKa shifts through metals: potential relevance to ribozyme chemistry. Chem Biodivers 5(8):1455–1474

Manalastas WW Jr, Dy ES, Quevada NP, Kasai H (2009) Trans-influence of nitrogen- and sulfur-containing ligands in trans-platinum complexes: a density functional theory study. J Phys Matter 21:064210/1–064210/6

Montero EI, Benedetti BT, Mangrum JB, Oehlsen MJ, Qu Y, Farrell NP (2007) Pre-association of polynuclear platinum anticancer agents on a protein, human serum albumin. Implications for drug design. Dalton Trans 43:4938–4942

Montero EI, Zhang J, Moniodis JJ, Berners-Price SJ, Farrel P (2010) The trans influence in the modulation of platinum anticancer agent biology: the effect of nitrite leaving group on aquation, reactions with S-nucleophiles and DNA binding of dinuclear and trinuclear compounds. Chem Eur J 16(30):9175–9185

Paolicchi A, Lorenzini E, Perego P, Supino R, Zunino F, Compòrti M, Pompella A (2002) Extra-cellular thiol metabolism in clones of human metastatic melanoma with different gamma-glutamyl transpeptidase expression: implications for cell response to platinum-based drugs. Int J Cancer 97(6):740–745

Peberdy JP, Malina J, Khalid S, Haman MJ, Rodger A (2007) Influence of surface shape on DNA binding of bimetallo helicates. J Inorg Biochem 101:1937–1945

Perdew JP, Chevary JA, Vosko SH, Jackson KA, Pederson MR, Sing DJ, Fiolhais C (1992) Atoms, molecules, solids, and surfaces: applications of the generalized gradient approximation for exchange and correlation. Phys Rev B 46(11):6671–6687

Pjura PE, Grzeskowiak K, Dickerson RE (1987) Binding of Hoechst 33258 to the minor groove of B-DNA. J Mol Biol 197(2):257–271

Podgorski I, Sloane BF (2003) Cathepsin B and its role(s) in cancer progression. Biochem Soc Symp 70:263–276

Roitzsch M, Añorbe MG, Miguel PJS, Müller B, Lippert B (2005) The role of intramolecular hydrogen bonding on nucleobase acidification following metal coordination: possible implications of an "indirect" role of metals in acid-base catalysis of nucleic acids. J Biol Inorg Chem 10(7):800–812

Ruiz J, Rodriguez V, de Haro C, Espinosa A, Perez J, Janiak C (2010) New 7-azaindole palladium and platinum complexes: crystal structures and theoretical calculations.

In vitro anticancer activity of the platinum compounds. Dalton Trans 39(13):3290–3301

Ruiz J, Vicente C, de Haro C, Bautista D (2013) Novel bis-C, N-cyclometalated iridium(III) thiosemicarbazide antitumor complexes: interactions with human serum albumin and DNA, and Inhibition of cathepsin B. Inorg Chem 52(2):974–982

Samper KG, Vicente C, Rodríguez V, Atrian S, Cutillas N, Capdevila M, Ruiz J, Palacios Ò (2012) Studying the interactions of a platinum(II) 9-aminoacridine complex with proteins and oligonucleotides by ESI-TOF MS. Dalton Trans 41(1):300–306

Spitznagel GW, Clark T, Chandrasekhar J, Schleyer PR (1982) Stabilization of methyl anions by first-row substituents. The superiority of diffuse function-augmented basis sets for anion calculations. J Comput Chem 3(3):3633–3640

Strojnik T, Kos J, Zidanik B, Golouh R, Lah T (1999) Cathepsin B immunohistochemical staining in tumor and endothelial cells is a new prognostic factor for survival in patients with brain tumors. Clin Cancer Res 5(3):559–567

te Velde G, Bickelhaupt FM, van Gisbergen SJA, Guerra CF, Baerends EJ, Snijders JG, Ziegler T (2001) Chemistry with ADF. J. Comp. Chem. 22(9):931–967

van Lenthe E, Ehlers AE, Baerends EJ (1999) Geometry optimizations in the zero order regular approximation for relativistic effects. J Chem Phys 110(18):8943–8953

Weisblum B, Haenssler E (1974) Fluorometric properties of the bibenzimidazole specific for AT [adenine-thymine] concentration in chromosomal DNA. Chromosoma 46(3): 255–260